

## DISEASES AND DISORDERS

# Gene expression signatures of target tissues in type 1 diabetes, lupus erythematosus, multiple sclerosis, and rheumatoid arthritis

F. Szymczak<sup>1,2\*</sup>, M. L. Colli<sup>1\*†</sup>, M. J. Mamula<sup>3</sup>, C. Evans-Molina<sup>4</sup>, D. L. Eizirik<sup>1,5†</sup>

Autoimmune diseases are typically studied with a focus on the immune system, and less attention is paid to responses of target tissues exposed to the immune assault. We presently evaluated, based on available RNA sequencing data, whether inflammation induces similar molecular signatures at the target tissues in type 1 diabetes, systemic lupus erythematosus, multiple sclerosis, and rheumatoid arthritis. We identified confluent signatures, many related to interferon signaling, indicating pathways that may be targeted for therapy, and observed a high (>80%) expression of candidate genes for the different diseases at the target tissue level. These observations suggest that future research on autoimmune diseases should focus on both the immune system and the target tissues, and on their dialog. Discovering similar disease-specific signatures may allow the identification of key pathways that could be targeted for therapy, including the repurposing of drugs already in clinical use for other diseases.

## INTRODUCTION

The incidence of autoimmune diseases is increasing on a worldwide basis, and the prevalence of some of the most severe autoimmune diseases, i.e., type 1 diabetes (T1D), systemic lupus erythematosus (SLE), multiple sclerosis (MS), and rheumatoid arthritis (RA), has reached levels of prevalence ranging from 0.5 to 5% in different regions of the world (1). There is no cure for these autoimmune diseases, which are characterized by the activation of the immune system against self-antigens. This is, in most cases, orchestrated by autoreactive B and T cells that trigger and drive tissue destruction in the context of local inflammation (2–5). While the immune targets of T1D, SLE, MS, and RA are distinct, they share several similar elements, including common variants that pattern disease risk, local inflammation with contribution by innate immunity, and downstream mechanisms mediating target tissue damage. In addition, disease courses are characterized by periods of aggressive autoimmune assaults followed by periods of decreased inflammation and partial recovery of the affected tissues (3, 6–11). Endoplasmic reticulum stress (12–15), reactive oxygen species (16–19), and inflammatory cytokines, such as interleukin-1 $\beta$  (IL-1 $\beta$ ) and interferons (IFNs), are also shared mediators of tissue damage in these pathologies (20–23).

Despite these common features, autoimmune disorders are traditionally studied independently and with a focus on the immune system rather than on the target tissues. There is increasing evidence that the target tissues of these diseases are not innocent bystanders of the autoimmune attack but participate in a deleterious dialog with the immune system that contributes to their own demise, as shown by our group and others in the case of T1D [reviewed in (3, 24, 25)]. Furthermore, in T1D, several of the risk genes for the disease seem to act at the target tissue level—in this case, pan-

creatic  $\beta$  cells—regulating the responses to “danger” signals, the dialog with the immune system, and apoptosis (20, 25, 26). Against this background, we hypothesize that key inflammation-induced mechanisms, potentially shared between T1D, SLE, MS, and RA, may drive similar molecular signatures at the target tissue level. Discovering these similar (or, in some cases, divergent) disease-specific signatures may allow the identification of key pathways that could be targeted for therapy, including the repurposing of drugs already in clinical use for other diseases.

To test this hypothesis, we obtained RNA sequencing (RNA-seq) datasets from pancreatic  $\beta$  cells from controls or individuals affected by T1D (27), from kidney cells from controls or individuals affected by SLE (28), from optic chiasm from controls or individuals affected by MS (29), and from joint tissue from controls or individuals affected by RA (30). In some cases, we also compared these datasets against our own datasets of cytokine-treated human  $\beta$  cells (31). These unique data were mined to identify similar and dissimilar gene signatures and to search for drugs that may potentially revert the observed signatures. Furthermore, we searched for the expression of candidate genes for the different autoimmune diseases at the target tissue level and the signaling pathways downstream of these candidate genes.

These studies indicate major common gene expression changes at the target tissues of the four autoimmune disease evaluated, many of them downstream of types I and II IFNs, and massive expression of candidate genes (>80% in all cases). These findings support the importance of studying the target tissue of autoimmune diseases, in dialog with the immune system, to better understand the genetics and natural history of these devastating diseases.

## RESULTS

### Metadata and global gene expression in the target tissues of different autoimmune diseases

The metadata of the tissue donors evaluated in the present analysis are shown in Table 1. The number of samples is proportional to the accessibility of the target tissues, with the highest number of samples available for joint tissue in RA. The age and sex of the patients reflect the natural history of the different diseases, with younger

Copyright © 2021  
The Authors, some  
rights reserved;  
exclusive licensee  
American Association  
for the Advancement  
of Science. No claim to  
original U.S. Government  
Works. Distributed  
under a Creative  
Commons Attribution  
NonCommercial  
License 4.0 (CC BY-NC).

<sup>1</sup>ULB Center for Diabetes Research, Medical Faculty, Université Libre de Bruxelles (ULB), Brussels, Belgium. <sup>2</sup>Interuniversity Institute of Bioinformatics in Brussels, Université Libre de Bruxelles-Vrije Universiteit Brussel, Brussels, Belgium. <sup>3</sup>Section of Rheumatology, Yale University School of Medicine, New Haven, CT, USA. <sup>4</sup>Center for Diabetes and Metabolic Diseases, Indiana University School of Medicine, Indianapolis, IN, USA. <sup>5</sup>Indiana Biosciences Research Institute (IBRI), Indianapolis, IN, USA.

\*These authors contributed equally to this work.

†Corresponding author. Email: mcolli@ulb.ac.be (M.L.C.); deizirik@ulb.ac.be (D.L.E.)

patients in the T1D group and a higher proportion of female patients in the MS and SLE groups. Sex information was obtained from the original metadata and, when not available, was inferred using chromosomal marker information present in the transcriptome (see Materials and Methods). Of note, while some of the samples used for RNA-seq were obtained following fluorescence-activated cell sorting (FACS) purification (e.g., pancreatic  $\beta$  cells) (27), other samples comprised a mixture of target cells and infiltrating immune cells. Determination of the leukocyte marker CD45 expression in the different samples indicated a trend for higher presence of immune-derived cells among samples obtained in T1D, MS, and RA, but not in SLE (table S1). This contribution by immune cells was, however, modest. For instance, while in the  $\beta$  cell preparation the number of transcripts per million (TPM) for CD45 in the patient group was 16.4 (mean), the TPM values for the following  $\beta$  cell markers were as follows: *INS* (Insulin), 125.359; Sodium/potassium-transporting ATPase gamma chain (*FXVD27a*), 65; *GCK* (Glucokinase), 20; Homeobox protein Nkx-2.2 (*NKX2-2*), 28; Synaptotagmin 4 (*SYT4*), 36; Neurogenic Differentiation 1 (*NEUROD1*), 27; Homeobox protein Nkx-6.1 (*NKX6-1*), 27; and MAF BZIP Transcription Factor B (*MAFB*), 23, indicating that the observed responses are driven, at least in part, by the constitutive cells of the target tissues. Of note, proinflammatory cytokines decrease the expression of several of the  $\beta$  cell markers (3, 20, 32) described above.

In the T1D and SLE datasets, but not in the MS and RA ones, there was a trend for more up-regulated than down-regulated genes in the target tissues, which was particularly marked in the T1D dataset, with more than twofold higher number of up-regulated genes as compared with the down-regulated ones (Fig. 1A). Of note, because of a statistically significant difference in the age of patients with RA and their respective controls, we have included age as an independent variable when determining the differentially expressed genes in the joint tissue samples (see Materials and Methods).

### Analysis of the gene patterns in target tissues of autoimmune diseases indicates up-regulation of IFN-related pathways

Enrichment analysis of these disease-modified genes (Fig. 1, B to E) indicated similarities and differences between the different autoimmune diseases. Thus, both T1D and SLE have several up-regulated IFN-related pathways among the top up-regulated ones (Fig. 1, B and C); IFN pathways were also detected as enriched for MS and RA, but not among the 20 top ones [e.g., MS: IFN- $\alpha\beta$  signaling normalized

enrichment score (NES) = 2.26 ( $P$  adj. < 0.007); RA, IFN- $\alpha\beta$  signaling NES = 2.64 ( $P$  adj. < 0.004)]. This similar enrichment in IFN-related genes can also explain the appearance of SLE as the top up-regulated pathway in T1D (Fig. 1B). Up-regulated pathways related to antigen presentation or antigen-related activation of immune cells were present for the four diseases (Fig. 1, B to E), in line with their autoimmune nature, while complement cascades were preeminent in MS (Fig. 1D) and RA (Fig. 1E), but less so in T1D and SLE. To evaluate whether these observed IFN-induced signatures originate, at least in part, from nonimmune cells in the target tissues, we reanalyzed available single-cell(sc)/nucleus(sn)-RNA-seq data focusing on nonimmune cells in affected tissues in T1D [pancreatic  $\beta$  cells (33)], SLE [kidney epithelial cells (34)], MS [brain neurons (35)], and RA [synovial fibroblasts (36)] (fig. S1A), confirming that there is a significant IFN signature in the target of the four autoimmune diseases as measured by an IFN response score, defined as the average expression of known IFN-stimulated genes (ISGs; see Materials and Methods) (34, 37).

The down-regulated pathways tended to be more disease specific and related to the dysfunction of the target organ. Thus, for T1D, there was down-regulation of pathways involved in “integration of energy metabolism,” a key step for insulin release, and in “regulation of gene expression in  $\beta$  cells,” which reflects the down-regulation of several transcription factors (TFs) critical for the maintenance of  $\beta$  cell phenotype and function (e.g., *PDX1* and *MAFA*) (38) (Fig. 1B), while in RA, there was a decrease in collagen chain trimerization, an important step for proper collagen folding (Fig. 1E) (39). Moreover, down-regulation of pathways involved in lipid metabolism was enriched in MS samples (Fig. 1D). Supporting that, disruption of lipid metabolism in oligodendrocytes compromises the lipid-rich myelin production/regeneration, a hallmark of MS, both in *in vitro* studies (40) and in samples obtained from individuals with MS (41).

Gene set enrichment analysis (GSEA) of the sc/sn-RNA-seq data of nonimmune cells from the four autoimmune diseases (fig. S1, B to E) confirmed several up-regulated pathways in common, including IFN signaling (present for all diseases, although not always among the top 20 shown), T1D (which appears in three of the four diseases), allograft rejection, etc. As observed in the bulk RNA-seq analysis, there were less similarities between diseases regarding the down-regulated pathways.

We also analyzed the intersection between significantly up- and down-regulated genes of the bulk RNA-seq of the four diseases using another criterion, namely, considering genes as significantly modified if they presented a false discovery rate <0.10 without a fold change

**Table 1. Summary of the metadata for the RNA-seq samples of the four autoimmune diseases.** RNA-seq data from four studies of target tissues in autoimmune diseases were retrieved from the Gene Expression Omnibus (GEO) portal (<https://ncbi.nlm.nih.gov/geo/>), reanalyzed, and quantified with Salmon using GENCODE 31 as the reference. N/A, data nonavailable. For the sex column: M, male; F, female.

Disease	Target tissue	Samples (n)		Age (mean $\pm$ SD)		Sex (n)		Source
		Patients	Controls	Patients	Controls	Patients	Controls	
T1D	Pancreatic $\beta$ cells	4	12	20.3 $\pm$ 5.6	16.1 $\pm$ 5.8	3 M/1 F	8 M/4 F	GSE121863 (27)
SLE	Kidney cells	20	7	~40	N/A	2 M/18 F*	7 F*	GSE98422 (28)
MS	Optic chiasm	5	5	56.2	57.6	5 F*	5 F*	GSE100297 (29)
RA	Joint tissue	57	28	55.9 $\pm$ 16.7	35.2 $\pm$ 16.2	33 F/24 M	14 F/14 M	GSE89408 (30)

\*Predicted using genes expressed in Y chromosome and XIST gene.

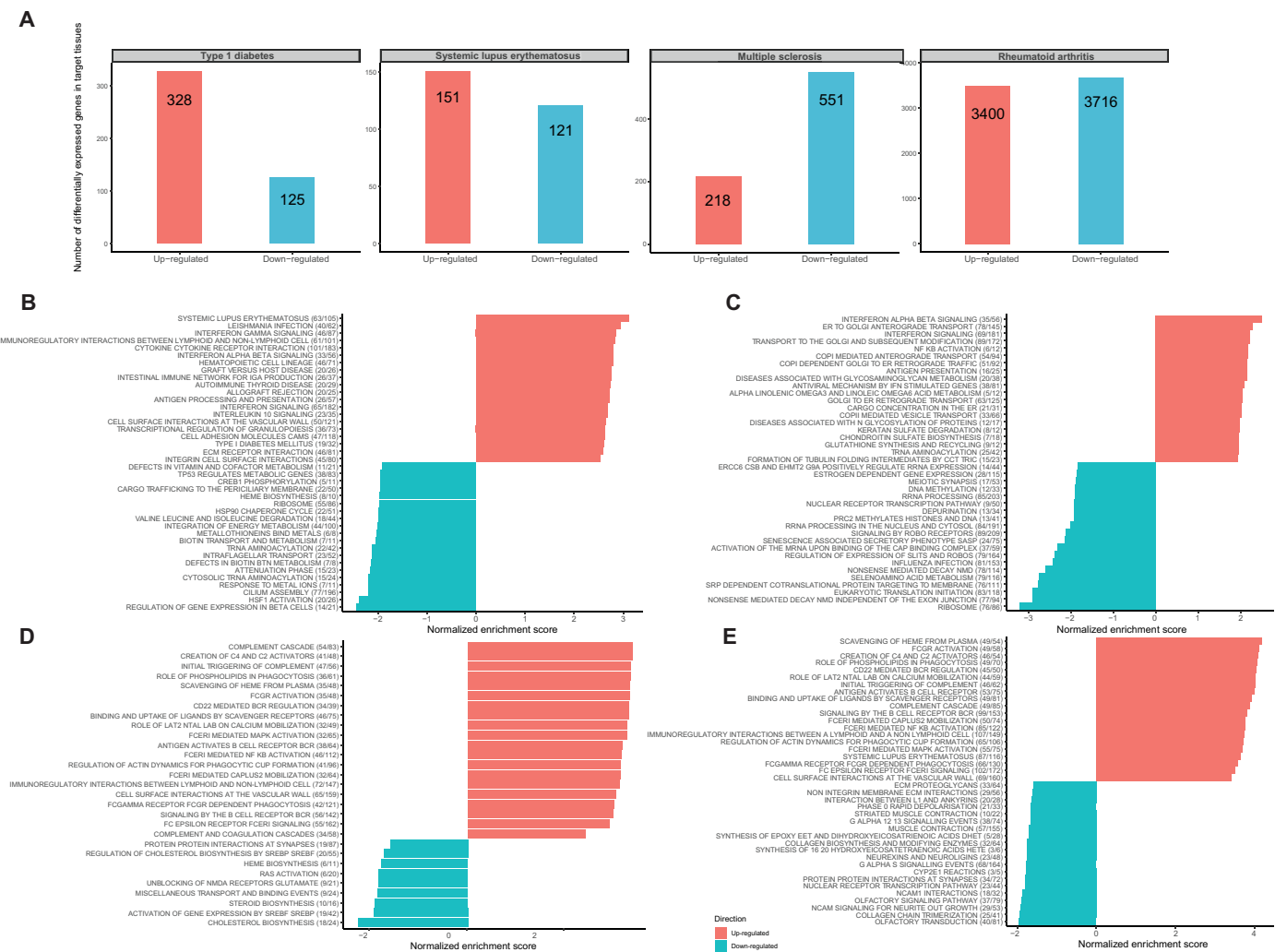


**Fig. 1. Overview of the number of differentially expressed genes and the signaling pathways activated in the target tissues of four autoimmune diseases.** (A) Number of protein-coding genes differentially expressed in four autoimmune diseases. Each RNA-seq data set was quantified with Salmon using GENCODE 31 as the reference. Differential expression was assessed with DESeq2. The numbers within the bars represent the protein-coding genes with |fold change| > 1.5 and an adjusted *P* value < 0.05. RNA-seq sample numbers (*n*) are as follows: T1D (*n* = 4 for patients, *n* = 10 for controls), SLE (*n* = 20 for patients, *n* = 7 for controls), MS (*n* = 5 for patients, *n* = 5 for controls), and RA (*n* = 56 for patients, *n* = 28 for controls). Results for the RA samples were adjusted by age as an independent variable. (B to E) Gene set enrichment analysis (GSEA) of T1D (B), SLE (C), MS (D), and RA (E) target tissues. After quantification using Salmon and differential expression with DESeq2, genes were ranked according to their fold change. Then, the fgSEA algorithm (76) was used along with the Kyoto Encyclopedia of Genes and Genomes (KEGG) and Reactome databases to determine significantly modified pathways. Bars in red and blue represent, respectively, a positive and negative enrichment in the associated pathway. The x axis shows the normalized enrichment score (NES) of the fgSEA analysis, and the y axis the enriched pathways. The numbers at the end of the signaling pathway names represent, respectively, (i) the number of genes present in the leading edge of the GSEA analysis and (ii) the total number of genes present in the gene set.

threshold (fig. S2, A and B). This showed a higher similarity among up- than down-regulated genes, but there were few genes in common between the four diseases. On the basis of a hypergeometric test to search for gene set enrichment for the cases where there were >50 genes in common between two and three diseases, we identified IFN signaling, antigen processing, and presentation and cytokine signaling, among others. It was, however, difficult to find common pathways among the down-regulated genes. A limitation of this approach is that we can only analyze genes that pass a fixed statistical cutoff, which makes the results very susceptible to the number of samples studied, as presently observed for the higher intersection between RA (a disease with a much higher number of samples) and the other autoimmune diseases. This type of analysis must thus

be redone as more samples become available for the different diseases.

To obtain more detailed information on the (dis)similarities between the different autoimmune diseases, avoiding the pitfalls mentioned above for threshold-based analysis, we performed the rank-rank hypergeometric overlap (RRHO) analysis (Fig. 2) (42), a genome-wide approach that compares two equally ranked datasets using a threshold-free algorithm (see Materials and Methods). The main similarities between the diseases were observed among up-regulated genes, while there was no major intersection of commonly down-regulated genes between datasets (Fig. 2). This finding is in line with the above-described observation that down-regulated genes tended to be target-tissue related (Fig. 1, B to E).  $\beta$  cells in



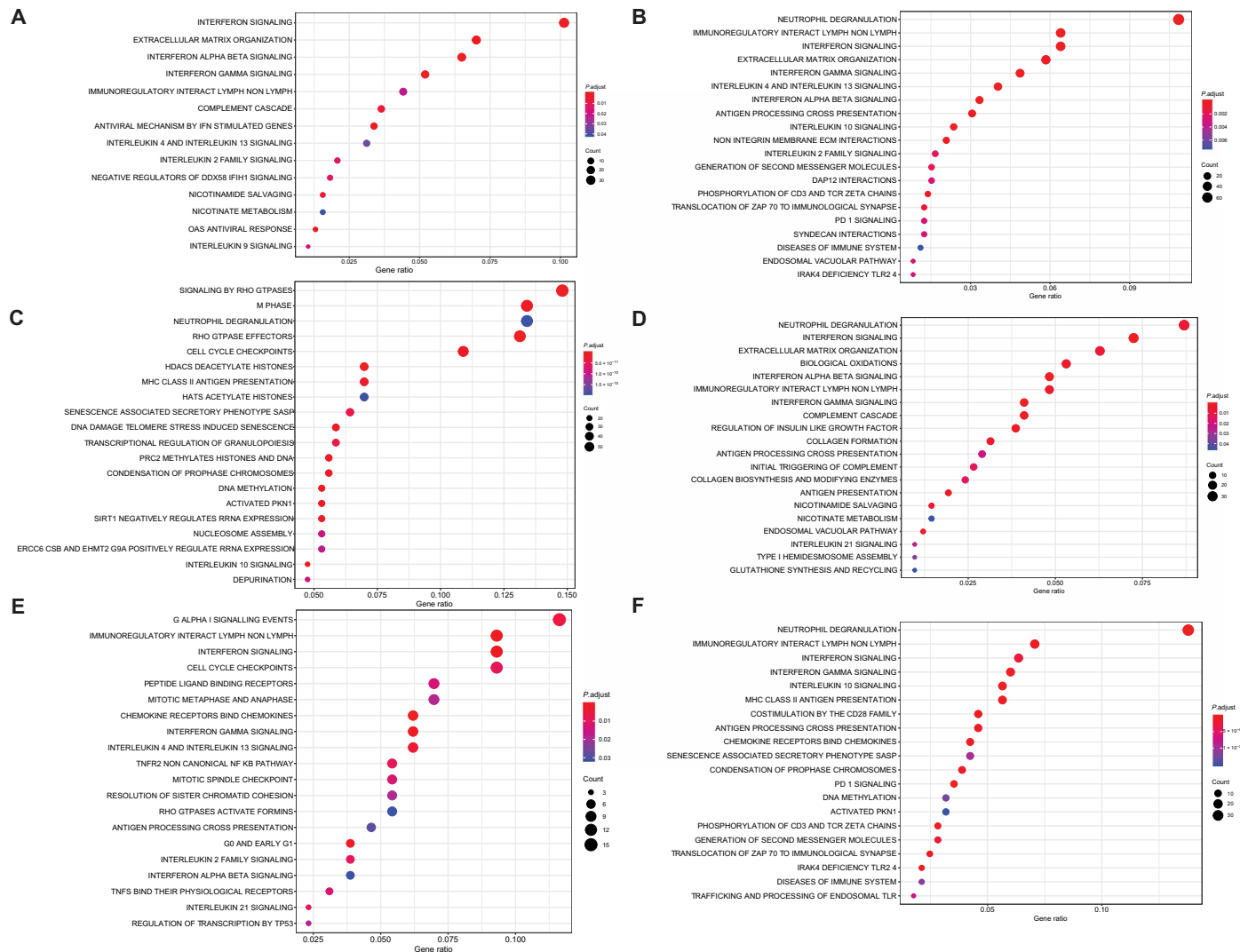


**Fig. 3. Functional enrichment analysis of overlapping genes among four autoimmune diseases demonstrates signaling pathways concordance.** (A to F) Genes significantly overlapping between different pairs of autoimmune diseases in the RRHO analysis (Fig. 2B) were selected for enrichment analysis using the clusterProfiler tool with the Reactome database. The top 20 gene sets are represented according to their adjusted *P* values (Benjamini and Hochberg correction) and their gene ratio (no. of modified genes/total gene set size). Diseases were analyzed in pairs. Enrichment analysis of genes significantly up-regulated in the target tissues of both (A) T1D and SLE, (B) T1D and MS, (C) T1D and RA, (D) SLE and MS, (E) SLE and RA, and (F) MS and RA.

I-BET-151, protect human  $\beta$  cells against the deleterious effects of IFN- $\alpha$  (31). There were additional interesting candidates, some with a profile covering multiple diseases, such as phosphoinositide 3-kinase (PI3K) (T1D versus SLE, SLE versus RA, and MS versus RA) and janus kinase (JAK) inhibitors (SLE versus RA and MS versus RA), while others acting on specific pairs of diseases, namely, bile acids (T1D versus MS) and fibroblast growth factor receptor (FGFR) inhibitors (SLE versus MS) (Fig. 4). Of note, clinical trials are currently evaluating the effects of the bile acid tauroursodeoxycholic acid (TUDCA) in patients with recent-onset T1D (ClinicalTrials.gov, NCT02218619) and MS (ClinicalTrials.gov, NCT03423121).

**Expression of candidate genes for the different autoimmune diseases at the target tissue level**

We have previously shown that isolated human pancreatic islets express a large number of risk genes for T1D (20, 24, 26, 48), and we

presently examined whether this is also the case for the target tissues in other autoimmune diseases (table S2). Confirming our previous findings, 81% of risk genes for T1D were expressed in human  $\beta$  cells; similar findings were observed for the target tissues for SLE (92%), MS (83%), and RA (88%). The autoimmune assault changed the expression of >65% of these candidate genes for joint tissue RA (table S2), but the number of disease-induced and significantly modified genes was much smaller for the other autoimmune diseases, probably because of limited statistical power associated to the number of samples analyzed (>80 samples studied in the case of RA and between 10 and 27 for the other diseases). The list of risk genes expressed in the target tissues is available in data file S1. An overview of these candidate genes and their coexpression in different autoimmune diseases is provided in Fig. 5. Genes related to antigen presentation [human lymphocyte antigen (*HLA*)-*DQB1* and *HLA-DRB1*] and to type I IFN signaling (*TYK2*) are present in all target tissues

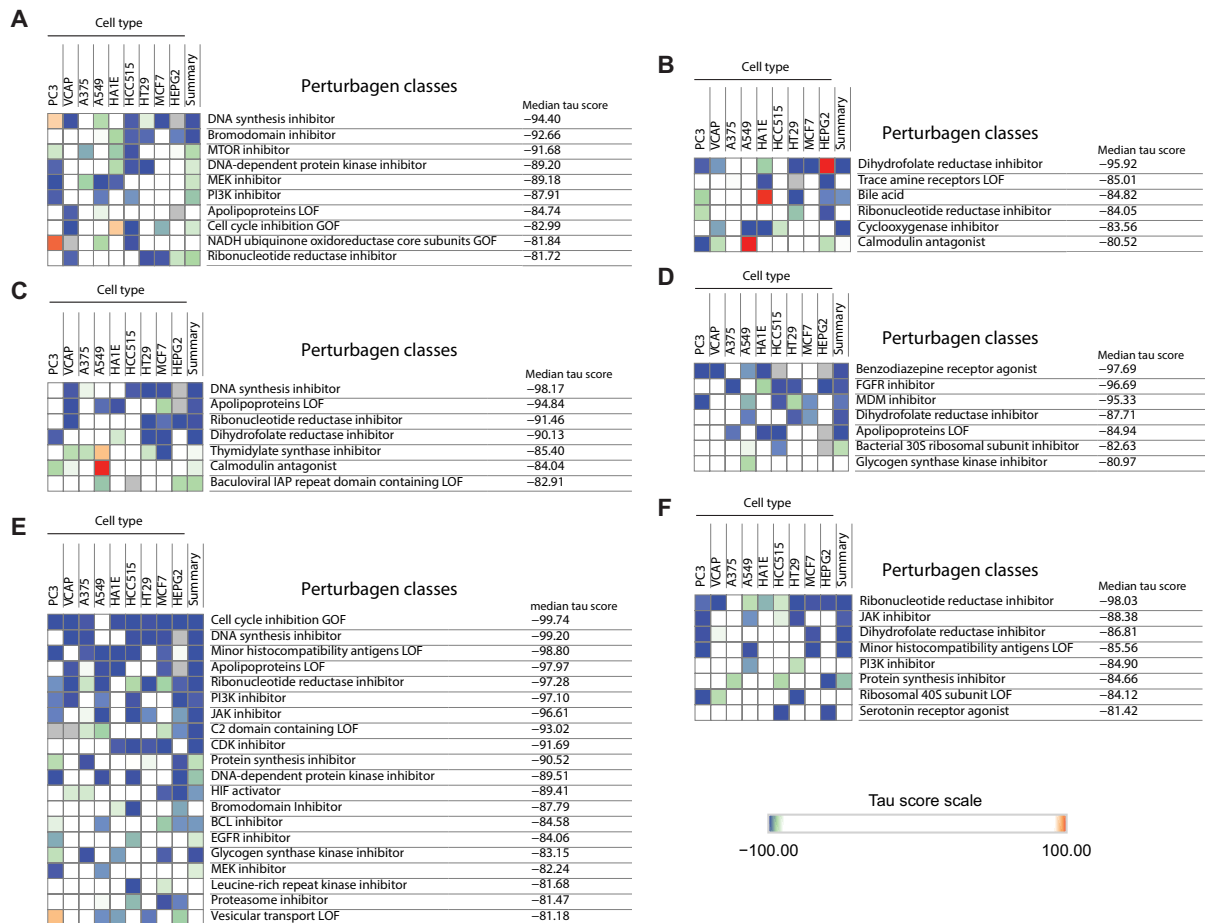


**Fig. 4. Mining overlapping genes among target tissues in four autoimmune diseases allows the identification of potential common therapeutic targets. (A to F)** After determining statistically which genes were overlapped in pairs of autoimmune diseases from the RRHO analysis (Fig. 2), the top 150 overlapping genes were submitted to the Connectivity Map database to identify perturbagen classes driving an opposite signature (negative tau score) to the one present in the target tissues of the four autoimmune diseases. Only classes with a median tau score  $\leq -80$  were considered. (A to F) Perturbagen classes driving down the genomic signatures of up-regulated genes. The same methodology and conditions have been applied for subsequent analysis: (A) T1D and SLE, (B) T1D and MS, (C) T1D and RA, (D) SLE and MS, (E) SLE and RA, and (F) MS and RA. EGFR, epidermal growth factor receptor; LOF, Loss of Function; GOS, Gain of Function; IAP, inhibitor of Apoptosis; FGFR, Fibroblast Growth Factor Receptor; MDM, Murine Double Minute; HIF, Hypoxia Inducible Factor; BCL, B-Cell Lymphoma.

for the four autoimmune diseases. Reactome (49) analysis of risk genes in T1D (data file S2) identified ILs and IFN signaling as important pathways. IFN signaling also appears pro-eminently for kidney tissue in SLE, optic chiasm in MS, and joint tissue in RA (data file S2), but there are also clusters related to defense against the autoimmune assault, including PD-1 (for all diseases) and IL-10 signaling (for SLE and MS only); PD-1–PDL1 (programmed death ligand 1) is probably also an important defense mechanism of human  $\beta$  cells in T1D (50).

To evaluate whether the observed candidate genes are expressed in nonimmune cells from the target tissues studied, we have used a similar approach as done for the TF analysis (fig. S3G) and revised sc/sn-RNA-seq data from nonimmune cells in affected tissues in T1D (33), SLE [kidney epithelial cells (34)], MS [brain neurons (35)], and RA [synovial fibroblasts (36)]. This confirmed that  $>80\%$  of the top 50 risk genes are expressed by the target cells (fig. S1, F to I). Of note, the present limitations of the sc-RNA-seq method regarding the number of genes detected (commented upon above) may explain why less candidate genes are observed in single cells (fig. S1, F to I) than in whole tissue or FACS-sorted bulk cells (data file S1).

## DISCUSSION

In the present study, we tested the hypothesis that target tissues from four different autoimmune diseases, namely, T1D, SLE, MS, and RA, engage in a “dialog” with the invading immune cells that leaves “molecular footprints.” These footprints may share similarities, as local inflammation is a common outcome of these diseases, and point to common mechanisms that can be targeted by therapy.

The analysis of the gene expression patterns of the target tissues in the different diseases showed up-regulation of type I and II IFN-related pathways, which is in line with observations made in the peripheral blood of individuals with T1D (51), SLE (52, 53), MS (54), and RA (55). These descriptive similarities were confirmed by comparing the ranking of the up-regulated genes via RRHO, a method that allows the comparison between differentially expressed genes in control and diseased tissue from two different diseases, outlining the similarities and/or dissimilarities between the modified genes in both diseases. Here, we observed clear but different degrees of overlap between the diseases mostly regarding the up-regulated expression



## Limitations

The study's first limitation relates to the scarcity of RNA-seq data for target tissues in autoimmune diseases, particularly in the cases where these tissues are difficult to access, such as in T1D or MS. This decreases the power of the analysis and may bias the data in favor of diseases where a larger number of samples were available (e.g., RA). Another issue is the stage of the disease, as the impact of the immune system on the target tissues may differ in the early and late phases of the disease [for instance, in the case of T1D, innate rather than adaptive immunity may have a major role at earlier stages (3, 25, 70)]. Unfortunately, and because of the scarcity of samples in, for instance, T1D or MS, this stage issue is difficult to address. It is noteworthy that despite these limitations, it was still possible to obtain clear conclusions from the available data.

Another potential limitation is that immune cells are present in the target tissue preparations analyzed (although there was a statistically significant increase in the expression of the immune marker CD45 only in T1D and RA), which may affect the gene expression pathways described above. The facts that (i) an IFN signature is present in nonimmune cells of the diseased tissues analyzed and these nonimmune cells express several candidate genes for the diseases studied (fig. S1); (ii) at least in the case of a pure human  $\beta$  cell line, EndoC- $\beta$ H1 cells, exposure to IFN- $\alpha$  induces a gene signature that is similar to that observed in  $\beta$  cells obtained from patients affected by T1D (31); and (iii) histological analysis of pancreatic islets from patients with T1D show expression of HLA class I (ABC) (71), *HLA-E* (31), *PDL1* (50), *CXCL10* (72), and *STAT1* (71) in pancreatic  $\beta$  cells, taken as a whole, suggest that at least part of the observed gene signatures originate from the target tissues and cannot be explained by the immune infiltration alone. Future follow-up studies based on direct histological staining of the specific cells involved are required to define the exact contribution of immune and nonimmune cells in the affected target tissues.

## MATERIALS AND METHODS

### Target tissue bulk RNA-seq processing and analysis

For each dataset, control and patient target tissue gene expressions were quantified using Salmon version 0.13.2 (73) with parameters “--seqBias --gcBias --validateMappings.” GENCODE version 31 (GRCh38) (74) was chosen as the reference genome and has been indexed with the default *k*-mer values. Differential expression was performed with DESeq2 version 1.24.0 (75). For each gene included in DESeq2's model, a log<sub>2</sub> fold change was computed and a Wald test statistic was assessed with a *P* value and an adjusted *P* value. In this study, we consider a gene as differentially expressed when |fold change| > 1.50 and adjusted *P* value < 0.05. Since there was a statistical difference in the age between patients with RA and controls, for this particular dataset, we have taken age as an independent variable in the general linear model performed by DESeq2. To introduce age as a confounding factor in the analysis, we performed a binning on the ages and assigned each donor a group, respectively: 10 to 29, 30 to 49, 50 to 69, and >70 years old. All the other parameters of the DESeq2 analysis were the same as for the others target tissues.

### sc/sn-RNA-seq processing and analysis

We have obtained the expression matrices containing the processed reads from transcriptome studies of the following target tissues: (i) sc-RNA-seq from cryo-banked islets obtained from three donors

with T1D and three controls matched for body mass index, age, sex, and storage time, performed using the SmartSeq-2 protocol as described in (33) and accessible under the Gene Expression Omnibus (GEO) number GSE124742; (ii) sc-RNA-seq from kidney biopsies from 24 patients with LN and 10 control samples acquired from living donor kidney biopsies using a modified CEL-Seq2 protocol as described in (34) and accessible in the ImmPort repository (accession code SDY997); (iii) sc-RNA-seq from snap-frozen brain tissue blocks obtained at autopsies from 10 patients with MS (1 primary progressive MS, 9 secondary progressive MS) and 9 nonaffected individuals processed using the 10x Genomics Single-Cell 3' system as described in (35) and accessible on Sequence Read Archive (SRA; accession number PRJNA544731); and (iv) sc-RNA-seq of synovial tissues from ultrasound-guided biopsies or joint replacements of 36 patients with RA and 15 patients with osteoarthritis, as reference controls, using the CEL-Seq2 protocol as described in (34) and available at ImmPort (accession code SDY998). After that, we normalized the gene expression levels by transforming the counts to log<sub>2</sub>(CPM + 1) (counts per million).

For the purpose of reproducibility, we have kept the same cell identity classification defined in the original sc/sn-RNA-seq study (33–36). To represent nonimmune cells on the target tissues, we have selected (i) in T1D, the  $\beta$  cells isolated from pancreatic islets; (ii) in SLE, all the kidney epithelial cells from the kidney biopsy; (iii) in MS, all the cells from different clusters of brain neurons; and (iv) in RA, all the cells from the fibroblast clusters of joint synovial tissues.

### Sex determination

For most, but not all, target tissues, sex information was available in the metadata on the GEO website. To compensate for this lack of information, we inferred the sex based on the expression of 40 genes exclusively coded on the Y chromosome and the female-expressed *XIST* (X-inactive specific transcript) (data file S1). We created a machine learning model on the basis of a linear discriminant analysis algorithm that we trained on the expression of both controls and patient expression matrices in RA. The training was supervised with the sex described in the metadata as the desired outcome. We then tried our model to predict the sex of patients on different target tissues (i.e., T1D and MS) where the outcome was known, according to their metadata, which provided only one prediction different from the expected outcome (96% accuracy). This allowed us to estimate the sex ratio in the studies missing this information in the available metadata.

### Risk genes

Risk genes associated with each disease were identified using genome-wide association study (GWAS) catalog ([www.ebi.ac.uk/gwas/](http://www.ebi.ac.uk/gwas/); consulted January 2020). The candidate genes were selected on the basis of the following criteria: (i) T1D, SLE, MA, and RA as the disease/trait evaluated by the study; (ii) a *P* value of  $< 0.5 \times 10^{-8}$  for the lead SNP; (iii) selecting the reported genes linked to the lead SNP described by the original study; and (iv) expression of the reported genes in the target tissue (TPM > 0.5). An overlap between the four lists of genes was then performed and represented as a Venn diagram.

### ISG score

To evaluate for the presence of types I and II IFN signatures on the target tissues of the four autoimmune diseases, we have calculated



for each cell from the sc/sn-RNA-seq an ISG score. This ISG score was calculated as the average expression of known ISGs listed on data file S1. The statistical difference between groups was determined using a two-tailed Mann-Whitney *U* test.

### RRHO analysis

To compare the genomic signatures of the target tissues of the four autoimmune diseases, we used an RRHO (42) mapping, an unbiased method to uncover the concordances and discordances between two similarly ranked lists. Briefly, for a pair of diseases, the full list of genes is ranked according to their fold change from the most down-regulated to the most up-regulated gene. Then, an intersection of shared genes is performed, and the analysis of the ranking order of genes is performed with a hypergeometric test.

The visual output of this analysis is an RRHO level map (Fig. 2A), where the hypergeometric *P* value for enrichment of *k* overlapping genes is calculated for all possible threshold pairs for each experiment, generating a matrix where the indices are the current rank in each experiment. *P* values for each test are then log transformed and reported on a heatmap to display the degrees of similarities according to four quadrants representing the concordance or the discordance in gene ranking in the two differential expression analysis (e.g., up-regulated in one disease and down-regulated in the other).

### Functional enrichment analysis

The functional enrichment analysis was based on results from the differential expression analysis. Genes from bulk RNA-seq data were pre-ranked according to the Wald test statistic of the differential expression results from DESeq2. For sc/sn-RNA-seq data, we filtered out genes that were expressed in less than 10% of all cells to minimize the dropout impact on the overall gene expression. The remaining genes were then preranked according to the log<sub>2</sub> fold change of the differential expression results from DESeq2. We used fGSEA (76) along with the Kyoto Encyclopedia of Genes and Genomes (KEGG) (77) and Reactome (49) databases as the references to determine which pathways were positively or negatively enriched in the target tissue of each disease. Default parameters were used, except for the number of permutations (10,000) for the most accurate *P* values. For bulk RNA-seq data, results with an adjusted *P* value <0.05 (Benjamini-Hochberg correction) were then sorted according to their NES. For sc/sn-RNA-seq data, results with an adjusted *P* value <0.15 (Benjamini-Hochberg correction) were then sorted according to their NES.

To determine the functional enrichment in genes up-regulated in pairs of diseases, we used a hypergeometric test included in the clusterProfiler package (78) on the genes overlapping significantly in the RRHO mapping. The Reactome (49) database was used as the reference for the gene sets. Default parameters were used, and *P* values were adjusted with the Benjamini-Hochberg correction.

### Venn diagrams

Genes differentially expressed with an adjusted *P* value <0.10 (Benjamini-Hochberg correction) were selected. The gene lists of all diseases were then overlapped and represented as a Venn diagram of up- or down-regulated genes. In case of an overlap of >50 genes, the gene list was processed using a hypergeometric test with the Reactome database as the reference. Default parameters were used, and *P* values were adjusted with the Benjamini-Hochberg correction.

### TF binding site analysis

Motif discovery for TF binding site in the promoter regions of up-regulated genes was done using the script findMotifs.pl from the HOMER (79) tools suite with parameters “-start -2000 -end 2000.” The promoter regions were considered as ±2000 base pairs from the gene transcription start site. Known TF binding site motifs uncovered and included in the study have a *P* value <0.05.

### Therapeutic target identification

For each RRHO analysis result, we picked the top 150 up-regulated genes shared between two diseases and processed this list with the Connectivity Map dataset (80) using the cloud-based CLUE software platform (<https://clue.io>). This allowed us to query the database for compounds that are driving down the input genomic signatures, revealing potential drugs that could be repurposed to treat one or more diseases. We focused then on perturbagen classes that displayed a negative median tau score and retained as potential drug candidates only classes with a median tau score <-80.

### Statistical analysis

TPM values are given according to their means ± SD. Results considered as significant in this study have a *P* value (or an adjusted *P* value when applicable) <0.05. For gene expression, we considered that a gene is differentially expressed if |fold change| >1.5 and adjusted *P* value <0.05, unless explicitly stated.

### SUPPLEMENTARY MATERIALS

Supplementary material for this article is available at <http://advances.sciencemag.org/cgi/content/full/7/2/eabd7600/DC1>

[View/request a protocol for this paper from Bio-protocol.](#)

### REFERENCES AND NOTES

- L. Fugger, L. T. Jensen, J. Rossjohn, Challenges, progress, and prospects of developing therapies to treat autoimmune diseases. *Cell* **181**, 63–80 (2020).
- P. L. Klarenbeek, M. J. H. de Hair, M. E. Doorenspleet, B. D. C. van Schaik, R. E. E. Esveldt, M. G. H. van de Sande, T. Cantaert, D. M. Gerlag, D. Baeten, A. H. C. van Kampen, F. Baas, P. P. Tak, N. de Vries, Inflamed target tissue provides a specific niche for highly expanded T-cell clones in early human autoimmune disease. *Ann. Rheum. Dis.* **71**, 1088–1093 (2012).
- D. L. Eizirik, M. L. Colli, F. Ortis, The role of inflammation in insulinitis and β-cell loss in type 1 diabetes. *Nat. Rev. Endocrinol.* **5**, 219–226 (2009).
- M. Kleinewietfeld, D. A. Hafler, Regulatory T cells in autoimmune neuroinflammation. *Immunol. Rev.* **259**, 231–244 (2014).
- E. F. McKinney, P. A. Lyons, E. J. Carr, J. L. Hollis, D. R. W. Jayne, L. C. Willcocks, M. Koukoulaki, A. Brazma, V. Jovanovic, D. M. Kemeny, A. J. Pollard, P. A. MacAry, A. N. Chaudhry, K. G. C. Smith, A CD8<sup>+</sup> T cell transcription signature predicts prognosis in autoimmune disease. *Nat. Med.* **16**, 586–591 (2010).
- E. Eller, P. Vardi, K. K. McFann, S. R. Babu, L. Yu, T. L. Bugawan, H. A. Erlich, G. S. Eisenbarth, P. R. Fain, Differential effects of DRB1\*0301 and DQA1\*0501-DQB1\*0201 on the activation and progression of islet cell autoimmunity. *Genes Immun.* **8**, 628–633 (2007).
- Y. Okada, D. Wu, G. Trynka, T. Raj, C. Terao, K. Ikari, Y. Kochi, K. Ohmura, A. Suzuki, S. Yoshida, R. R. Graham, A. Manoharan, W. Ortmann, T. Bhargava, J. C. Denny, R. J. Carroll, A. E. Eyler, J. D. Greenberg, J. M. Kremer, D. A. Pappas, L. Jiang, J. Yin, L. Ye, D.-F. Su, J. Yang, G. Xie, E. Keystone, H.-J. Westra, T. Esko, A. Metspalu, X. Zhou, N. Gupta, D. Mirel, E. A. Stahl, D. Diogo, J. Cui, K. Liao, M. H. Guo, K. Myouzen, T. Kawaguchi, M. J. H. Coenen, P. L. C. M. van Riel, M. A. F. J. van de Laar, H.-J. Guchelaar, T. W. J. Huizinga, P. Dieudé, X. Mariette, S. Louis Bridges Jr., A. Zhernakova, R. E. M. Toes, P. P. Tak, C. Miceli-Richard, S.-Y. Bang, H.-S. Lee, J. Martin, M. A. Gonzalez-Gay, L. Rodriguez-Rodriguez, S. Rantapää-Dahlqvist, L. Årlestig, H. K. Choi, Y. Kamatani, P. Galan, M. Lathrop; RACI consortium; GARNET consortium, S. Eyre, J. Bowes, A. Barton, N. de Vries, L. W. Moreland, L. A. Criswell, E. W. Karlson, A. Taniguchi, R. Yamada, M. Kubo, J. S. Liu, S.-C. Bae, J. Worthington, L. Padyukov, L. Klareskog, P. K. Gregersen, S. Raychaudhuri, B. E. Stranger, P. L. De Jager, L. Franke, P. M. Visscher, M. A. Brown, H. Yamanaka, T. Mimori, A. Takahashi, H. Xu, T. W. Behrens, K. A. Siminovitsh, S. Momohara, F. Matsuda, K. Yamamoto, R. M. Plenge, Genetics of rheumatoid arthritis contributes to biology and drug discovery. *Nature* **506**, 376–381 (2014).

8. C. M. Weyand, K. C. Hicok, D. L. Conn, J. J. Goronzy, The influence of HLA-DRB1 genes on disease severity in rheumatoid arthritis. *Ann. Intern. Med.* **117**, 801–806 (1992).
9. S. Viatte, J. C. Lee, B. Fu, M. Espéli, M. Lunt, J. N. E. De Wolf, L. Wheeler, J. A. Reynolds, M. Castelino, D. P. M. Symmons, P. A. Lyons, A. Barton, K. G. C. Smith, Association between genetic variation in *FOXO3* and reductions in inflammation and disease activity in inflammatory polyarthritis. *Arthritis Rheumatol.* **68**, 2629–2636 (2016).
10. M.-L. Yang, H. A. Doyle, S. G. Clarke, K. C. Herold, M. J. Mamula, Oxidative modifications in tissue pathology and autoimmune disease. *Antioxid. Redox Signal.* **29**, 1415–1431 (2018).
11. M. I. Alvelos, J. Juan-Mateu, M. L. Colli, J.-V. Turatsinze, D. L. Eizirik, When one becomes many – Alternative splicing in  $\beta$ -cell function and failure. *Diabetes Obes. Metab.* **20**, 77–87 (2018).
12. D. L. Eizirik, M. Cnop, ER stress in pancreatic  $\beta$  cells: The thin red line between adaptation and failure. *Sci. Signal.* **3**, pe7 (2010).
13. Q. Cheng, X. Wang, Y. Shen, Y. Shen, B. Zu, J. Xu, Y. Xu, X. Zuo, Q. Cheng, J. Wang, Deficiency of IRE1 and PERK signal pathways in systemic lupus erythematosus. *Am. J. Med. Sci.* **348**, 465–473 (2014).
14. M. Rahmati, M. A. Moosavi, M. F. McDermott, ER stress: A therapeutic target in rheumatoid arthritis? *Trends Pharmacol. Sci.* **39**, 610–623 (2018).
15. S. Stone, W. Lin, The unfolded protein response in multiple sclerosis. *Front. Neurosci.* **9**, 264 (2015).
16. E. Balogh, D. J. Veale, T. McGarry, C. Orr, Z. Szekanecz, C.-T. Ng, U. Fearon, M. Biniecka, Oxidative stress impairs energy metabolism in primary cells and synovial tissue of patients with rheumatoid arthritis. *Arthritis Res. Ther.* **20**, 95 (2018).
17. K. Ohl, K. Tenbrock, M. Kipp, Oxidative stress in multiple sclerosis: Central and peripheral mode of action. *Exp. Neurol.* **277**, 58–67 (2016).
18. J. Chen, S. E. Stimpson, G. A. Fernandez-Bueno, C. E. Mathews, Mitochondrial reactive oxygen species and type 1 diabetes. *Antioxid. Redox Signal.* **29**, 1361–1372 (2018).
19. D. Shah, N. Mahajan, S. Sah, S. K. Nath, B. Paudyal, Oxidative stress and its biomarkers in systemic lupus erythematosus. *J. Biomed. Sci.* **21**, 23 (2014).
20. D. L. Eizirik, M. Sammeth, T. Bouckennooghe, G. Bottu, G. Sisino, M. Igoillo-Estevé, F. Ortis, I. Santin, M. L. Colli, J. Barthson, L. Bouwens, L. Hughes, L. Gregory, G. Lunter, L. Marselli, P. Marchetti, M. I. McCarthy, M. Cnop, The human pancreatic islet transcriptome: Expression of candidate genes for type 1 diabetes and the impact of pro-inflammatory cytokines. *PLoS Genet.* **8**, e1002552 (2012).
21. J. A. Reynolds, E. M. McCarthy, S. Haque, P. Ngamjanyaporn, J. C. Sergeant, E. Lee, E. Lee, S. A. Kilfeather, B. Parker, I. N. Bruce, Cytokine profiling in active and quiescent SLE reveals distinct patient subpopulations. *Arthritis Res. Ther.* **20**, 173 (2018).
22. T. Khaibullin, V. Ivanova, E. Martynova, G. Cherepnev, F. Khabirov, E. Granatov, A. Rizvanov, S. Khaiboullina, Elevated levels of proinflammatory cytokines in cerebrospinal fluid of multiple sclerosis patients. *Front. Immunol.* **8**, 531 (2017).
23. S. Mateen, S. Moin, S. Shahzad, A. Q. Khan, Level of inflammatory cytokines in rheumatoid arthritis patients: Correlation with 25-hydroxy vitamin D and reactive oxygen species. *PLoS ONE* **12**, e0178879 (2017).
24. A. Op de Beek, D. L. Eizirik, Viral infections in type 1 diabetes mellitus—Why the  $\beta$  cells? *Nat. Rev. Endocrinol.* **12**, 263–273 (2016).
25. D. L. Eizirik, L. Pasquali, M. Cnop, Pancreatic  $\beta$ -cells in type 1 and type 2 diabetes mellitus: Different pathways to failure. *Nat. Rev. Endocrinol.* **16**, 349–362 (2020).
26. M. Ramos-Rodríguez, H. Raurcell-Vila, M. L. Colli, M. I. Alvelos, M. Subirana-Granés, J. Juan-Mateu, R. Norris, J.-V. Turatsinze, E. S. Nakayasu, B.-J. M. Webb-Robertson, J. R. J. Inshah, P. Marchetti, L. Piemonti, M. Esteller, J. A. Todd, T. O. Metz, D. L. Eizirik, L. Pasquali, The impact of proinflammatory cytokines on the  $\beta$ -cell regulatory landscape provides insights into the genetics of type 1 diabetes. *Nat. Genet.* **51**, 1588–1595 (2019).
27. M. A. Russell, S. D. Redick, D. M. Blodgett, S. J. Richardson, P. Leete, L. Krogvold, K. Dahl-Jørgensen, R. Bottino, M. Brissova, J. M. Spaeth, J. A. B. Babon, R. Haliyur, A. C. Powers, C. Yang, S. C. Kent, A. G. Derr, A. Kucukural, M. G. Garber, N. G. Morgan, D. M. Harlan, HLA class II antigen processing and presentation pathway components demonstrated by transcriptome and protein analyses of islet  $\beta$ -cells from donors with type 1 diabetes. *Diabetes* **68**, 988–1001 (2019).
28. Z. Liao, Z. Ye, Z. Xue, L. Wu, Y. Ouyang, C. Yao, C. Cui, N. Xu, J. Ma, G. Hou, J. Wang, Y. Meng, Z. Yin, Y. Liu, J. Qian, C. Zhang, H. Ding, Q. Guo, B. Qu, N. Shen, Identification of renal long non-coding RNA RP11-2B6.2 as a positive regulator of type I interferon signaling pathway in lupus nephritis. *Front. Immunol.* **10**, 975 (2019).
29. N. Itoh, Y. Itoh, A. Tassoni, E. Ren, M. Kaito, A. Ohno, Y. Ao, V. Farkhondeh, H. Johnsonbaugh, J. Burda, M. V. Sofroniew, R. R. Voskuhl, Cell-specific and region-specific transcriptomics in the multiple sclerosis model: Focus on astrocytes. *Proc. Natl. Acad. Sci. U.S.A.* **115**, E302–E309 (2018).
30. Y. Guo, A. M. Walsh, U. Fearon, M. D. Smith, M. D. Wechalekar, X. Yin, S. Cole, C. Orr, T. McGarry, M. Canavan, S. Kelly, T.-A. Lin, X. Liu, S. M. Proudman, D. J. Veale, C. Pitzalis, S. Nagpal, CD40L-dependent pathway is active at various stages of rheumatoid arthritis disease progression. *J. Immunol.* **198**, 4490–4501 (2017).
31. M. L. Colli, M. Ramos-Rodríguez, E. S. Nakayasu, M. I. Alvelos, M. Lopes, J. L. E. Hill, J.-V. Turatsinze, A. C. de Brachène, M. A. Russell, H. Raurcell-Vila, A. Castela, J. Juan-Mateu, B.-J. M. Webb-Robertson, L. Krogvold, K. Dahl-Jørgensen, L. Marselli, P. Marchetti, S. J. Richardson, N. G. Morgan, T. O. Metz, L. Pasquali, D. L. Eizirik, An integrated multi-omics approach identifies the landscape of interferon- $\alpha$ -mediated responses of human pancreatic beta cells. *Nat. Commun.* **11**, 2584 (2020).
32. S. Usmani-Brown, A. L. Perdigoto, N. Lavoie, P. Clark, M. Korah, J. Rui, G. Betancur, K. C. Herold,  $\beta$  cell responses to inflammation. *Mol. Metab.* **27**, S104–S113 (2019).
33. J. Camunas-Soler, X.-Q. Dai, Y. Hang, A. Bautista, J. Lyon, K. Suzuki, S. K. Kim, S. R. Quake, P. E. MacDonald, Patch-seq links single-cell transcriptomes to human islet dysfunction in diabetes. *Cell Metab.* **31**, 1017–1031.e4 (2020).
34. A. Arazi, D. A. Rao, C. C. Berthier, A. Davidson, Y. Liu, P. J. Hoover, A. Chicoine, T. M. Eisenhaure, A. H. Jonsson, S. Li, D. J. Lieb, F. Zhang, K. Slowikowski, E. P. Browne, A. Noma, D. Sutherby, S. Steelman, D. E. Smilek, P. Tosta, W. Apruzzese, E. Massarotti, M. Dall’Era, M. Park, D. L. Kamen, R. A. Furie, F. Payan-Schober, W. F. Pendergraft, E. A. McInnis, J. P. Buyon, M. A. Petri, C. Putterman, K. C. Kalunian, E. S. Woodle, J. A. Lederer, D. A. Hildeman, C. Nusbaum, S. Raychaudhuri, M. Kretzler, J. H. Anolik, M. B. Brenner, D. Wofsy, N. Hacohen, B. Diamond; Accelerating Medicines Partnership in SLE network. The immune cell landscape in kidneys of patients with lupus nephritis. *Nat. Immunol.* **20**, 902–914 (2019).
35. L. Schirmer, D. Velmeshev, S. Holmqvist, M. Kaufmann, S. Werneburg, D. Jung, S. Vistnes, J. H. Stockley, A. Young, M. Steindel, B. Tung, N. Goyal, A. Bhaduri, S. Mayer, J. B. Engler, O. A. Bayraktar, R. J. M. Franklin, M. Haussler, R. Reynolds, D. P. Schafer, M. A. Friese, L. R. Shioh, A. R. Kriegstein, D. H. Rowitch, Neuronal vulnerability and multilineage diversity in multiple sclerosis. *Nature* **573**, 75–82 (2019).
36. F. Zhang, K. Wei, K. Slowikowski, C. Y. Fonseka, D. A. Rao, S. Kelly, S. M. Goodman, D. Tabechian, L. B. Hughes, K. Salomon-Escoto, G. F. M. Watts, A. H. Jonsson, J. Rangel-Moreno, N. Meednu, C. Roza, W. Apruzzese, T. M. Eisenhaure, D. J. Lieb, D. L. Boyle, A. M. Mandelin II; Accelerating Medicines Partnership Rheumatoid Arthritis and Systemic Lupus Erythematosus (AMP RA/SLE) Consortium, B. F. Boyce, E. DiCarlo, E. M. Gravalles, P. K. Gregersen, L. Moreland, G. S. Firestein, N. Hacohen, C. Nusbaum, J. A. Lederer, H. Perlman, C. Pitzalis, A. Filer, V. M. Holers, V. P. Bykerk, L. T. Donlin, J. H. Anolik, M. B. Brenner, S. Raychaudhuri, Defining inflammatory cell states in rheumatoid arthritis joint synovial tissues by integrating single-cell transcriptomics and mass cytometry. *Nat. Immunol.* **20**, 928–942 (2019).
37. L. Chiche, N. Jourde-Chiche, E. Whalen, S. Presnell, V. Gersuk, K. Dang, E. Anguiano, C. Quinn, S. Burtay, Y. Berland, G. Kaplanski, J.-R. Harle, V. Pascual, D. Chaussabel, Modular transcriptional repertoire analyses of adults with systemic lupus erythematosus reveal distinct type I and type II interferon signatures. *Arthritis Rheumatol.* **66**, 1583–1595 (2014).
38. J. M. Spaeth, E. M. Walker, R. Stein, Impact of Pdx1-associated chromatin modifiers on islet  $\beta$ -cells. *Diabetes Obes. Metab.* **18**, 123–127 (2016).
39. S. P. Boudko, J. Engel, H. P. Bächinger, The crucial role of trimerization domains in collagen folding. *Int. J. Biochem. Cell Biol.* **44**, 21–32 (2012).
40. H. Monnerie, M. Romer, B. K. Jensen, J. S. Millar, K. L. Jordan-Sciutto, S. F. Kim, M. B. Grinspan, Reduced sterol regulatory element-binding protein (SREBP) processing through site-1 protease (S1P) inhibition alters oligodendrocyte differentiation in vitro. *J. Neurochem.* **140**, 53–67 (2017).
41. X. Zhou, C. He, J. Ren, C. Dai, S. R. Stevens, Q. Wang, D. Zamler, T. Shingu, L. Yuan, C. R. Chandregowda, Y. Wang, V. Ravikummar, A. U. K. Rao, F. Zhou, H. Zheng, M. N. Rasband, Y. Chen, F. Lan, A. B. Heimberger, B. M. Segal, J. Hu, Mature myelin maintenance requires Klf1 to coactivate PPAR $\beta$ -RXR $\alpha$ -mediated lipid metabolism. *J. Clin. Invest.* **130**, 2220–2236 (2020).
42. S. B. Plaisier, R. Taschereau, J. A. Wong, T. G. Graeber, Rank–rank hypergeometric overlap: Identification of statistically significant overlap between gene-expression signatures. *Nucleic Acids Res.* **38**, e169 (2010).
43. M. D. Luecken, F. J. Theis, Current best practices in single-cell RNA-seq analysis: A tutorial. *Mol. Syst. Biol.* **15**, e8746 (2019).
44. L. C. Tsoi, G. A. Hile, C. C. Berthier, M. K. Sarkar, T. J. Reed, J. Liu, R. Uppala, M. Patrick, K. Raja, X. Xing, E. Xing, K. He, J. E. Gudjonsson, J. M. Kahlenberg, Hypersensitive IFN responses in lupus keratinocytes reveal key mechanistic determinants in cutaneous lupus. *J. Immunol.* **202**, 2121–2130 (2019).
45. P. Mistry, S. Nakabo, L. O’Neil, R. R. Goel, K. Jiang, C. Carmona-Rivera, S. Gupta, D. W. Chan, P. M. Carlucci, X. Wang, F. Naz, Z. Manna, A. Dey, N. N. Mehta, S. Hasni, S. Dell’Orso, G. Gutierrez-Cruz, H.-W. Sun, M. J. Kaplan, Transcriptomic, epigenetic, and functional analyses implicate neutrophil diversity in the pathogenesis of systemic lupus erythematosus. *Proc. Natl. Acad. Sci. U.S.A.* **116**, 25222–25228 (2019).
46. B. N. Cronstein, T. M. Aune, Methotrexate and its mechanisms of action in inflammatory arthritis. *Nat. Rev. Rheumatol.* **16**, 145–154 (2020).
47. A. Fanouraki, M. Kostopoulou, A. Alunno, M. Aringer, I. Bajema, J. N. Boletis, R. Cervera, A. Doria, C. Gordon, M. Govoni, F. Houssiau, D. Jayne, M. Kouloumas, A. Kuhn, J. L. Larsen, K. Lerstrøm, G. Moroni, M. Mosca, M. Schneider, J. S. Smolen, E. Svenungsson, V. Tesar, A. Tincani, A. Toldborg, R. van Vollenhoven, J. Wenzel, G. Bertias, D. T. Boumpas, 2019 update of the EULAR recommendations for the management of systemic lupus erythematosus. *Ann. Rheum. Dis.* **78**, 736–745 (2019).

48. L. Marroqui, R. S. Dos Santos, A. O. de Beeck, A. C. de Brachène, L. Marselli, P. Marchetti, D. L. Eizirik, Interferon- $\alpha$  mediates human beta cell HLA class I overexpression, endoplasmic reticulum stress and apoptosis, three hallmarks of early human type 1 diabetes. *Diabetologia* **60**, 656–667 (2017).
49. A. Fabregat, S. Jupe, L. Matthews, K. Sidiropoulos, M. Gillespie, P. Garapati, R. Haw, B. Jassal, F. Korninger, B. May, M. Milacic, C. D. Roca, K. Rothfels, C. Sevilla, V. Shamovsky, S. Shorser, T. Varusai, G. Viteri, G. Weiser, G. Wu, L. Stein, H. Hermjakob, P. D'Eustachio, The Reactome pathway knowledgebase. *Nucleic Acids Res.* **46**, D649–D655 (2018).
50. M. L. Colli, J. L. E. Hill, L. Marroqui, J. Chaffey, R. S. Dos Santos, P. Leete, A. Coomans de Brachène, F. M. M. Paula, A. Op de Beeck, A. Castela, L. Marselli, L. Krogvold, K. Dahl-Jørgensen, P. Marchetti, N. G. Morgan, S. J. Richardson, D. L. Eizirik, PDL1 is expressed in the islets of people with type 1 diabetes and is up-regulated by interferons- $\alpha$  and  $\gamma$  via IRF1 induction. *EBioMedicine* **36**, 367–375 (2018).
51. R. C. Ferreira, H. Guo, R. M. R. Coulson, D. J. Smyth, M. L. Pekalski, O. S. Burren, A. J. Cutler, J. D. Doecke, S. Flint, E. F. McKinney, P. A. Lyons, K. G. C. Smith, P. Achenbach, A. Beyerlein, D. B. Dunger, D. G. Clayton, L. S. Wicker, J. A. Todd, E. Bonifacio, C. Wallace, A.-G. Ziegler, A type I interferon transcriptional signature precedes autoimmunity in children genetically at risk for type 1 diabetes. *Diabetes* **63**, 2538–2550 (2014).
52. A. M. Becker, K. H. Dao, B. K. Han, R. Kornu, S. Lakhanpal, A. B. Mobley, Q.-Z. Li, Y. Lian, T. Wu, A. M. Reimold, N. J. Olsen, D. R. Karp, F. Z. Chowdhury, J. D. Farrar, A. B. Satterthwaite, C. Mohan, P. E. Lipsky, E. K. Wakeland, L. S. Davis, SLE peripheral blood B cell, T cell and myeloid cell transcriptomes display unique profiles and each subset contributes to the interferon signature. *PLoS ONE* **8**, e67003 (2013).
53. M. K. Crow, Type I interferon in the pathogenesis of lupus. *J. Immunol.* **192**, 5459–5468 (2014).
54. S. Srinivasan, M. Severa, F. Rizzo, R. Menon, E. Brini, R. Mechelli, V. Martinelli, P. Hertzog, M. Salvetti, R. Furlan, G. Martino, G. Comi, E. M. Coccia, C. Farina, Transcriptional dysregulation of interferome in experimental and human multiple sclerosis. *Sci. Rep.* **7**, 8981 (2017).
55. T. D. de Jong, J. Lübbers, S. Turk, S. Vosslander, E. Mantel, H. J. Bontkes, C. J. van der Laken, J. W. Bijlsma, D. van Schaardenburg, C. L. Verweij, The type I interferon signature in leukocyte subsets from peripheral blood of patients with early arthritis: A major contribution by granulocytes. *Arthritis Res. Ther.* **18**, 165 (2016).
56. P. C. Taylor, Clinical efficacy of launched JAK inhibitors in rheumatoid arthritis. *Rheumatology* **58**, i17–i26 (2019).
57. D. J. Wallace, R. A. Furie, Y. Tanaka, K. C. Kalunian, M. Mosca, M. A. Petri, T. Dörner, M. H. Cardiel, I. N. Bruce, E. Gomez, T. Carmack, A. M. DeLozier, J. M. Janes, M. D. Linnik, S. de Bono, M. E. Silk, R. W. Hoffman, Baricitinib for systemic lupus erythematosus: A double-blind, randomised, placebo-controlled, phase 2 trial. *Lancet* **392**, 222–231 (2018).
58. P. M. Trivedi, K. L. Graham, N. A. Scott, M. R. Jenkins, S. Majaw, R. M. Sutherland, S. Fynch, A. M. Lew, C. J. Burns, B. Krishnamurthy, T. C. Brodnicki, S. I. Manning, T. W. Kay, H. E. Thomas, Repurposed JAK1/JAK2 inhibitor reverses established autoimmune insulinitis in NOD mice. *Diabetes* **66**, 1650–1660 (2017).
59. H. Li, D. Park, P. M. Abdul-Muneer, B. Xu, H. Wang, B. Xing, D. Wu, S. Li, PI3K $\gamma$  inhibition alleviates symptoms and increases axon number in experimental autoimmune encephalomyelitis mice. *Neuroscience* **253**, 89–99 (2013).
60. D. F. Barber, A. Bartolomé, C. Hernandez, J. M. Flores, C. Redondo, C. Fernandez-Arias, M. Camps, T. Rückle, M. K. Schwarz, S. Rodriguez, C. Martinez-A, D. Balomenos, C. Rommel, A. C. Carrera, PI3K $\gamma$  inhibition blocks glomerulonephritis and extends lifespan in a mouse model of systemic lupus. *Nat. Med.* **11**, 933–935 (2005).
61. M. Camps, T. Rückle, H. Ji, V. Ardisson, F. Rintelen, J. Shaw, C. Ferrandi, C. Chabert, C. Gillieron, B. Françon, T. Martin, D. Gretener, D. Perrin, D. Leroy, P.-A. Vitte, E. Hirsch, M. P. Wymann, R. Cirillo, M. K. Schwarz, C. Rommel, Blockade of PI3K $\gamma$  suppresses joint inflammation and damage in mouse models of rheumatoid arthritis. *Nat. Med.* **11**, 936–943 (2005).
62. M. Reinwald, J. T. Silva, N. J. Mueller, J. Fortún, C. Garzoni, J. W. de Fijter, M. Fernández-Ruiz, P. Grossi, J. M. Aguado, ESCMID Study Group for Infections in Compromised Hosts (ESGICH) Consensus Document on the safety of targeted and biological therapies: An infectious diseases perspective (Intracellular signaling pathways: Tyrosine kinase and mTOR inhibitors). *Clin. Microbiol. Infect.* **24**, S53–S70 (2018).
63. A. C. Grammer, M. M. Ryals, S. E. Heuer, R. D. Robl, S. Madamanchi, L. S. Davis, B. Lauwerys, M. D. Catalina, P. E. Lipsky, Drug repositioning in SLE: Crowd-sourcing, literature-mining and big data analysis. *Lupus* **25**, 1150–1170 (2016).
64. M. Zhang, H. Luo, Z. Xi, E. Rogava, Drug repositioning for diabetes based on “omics” data mining. *PLoS ONE* **10**, e0126082 (2015).
65. T. T. Ashburn, K. B. Thor, Drug repositioning: Identifying and developing new uses for existing drugs. *Nat. Rev. Drug Discov.* **3**, 673–683 (2004).
66. I. Santin, D. L. Eizirik, Candidate genes for type 1 diabetes modulate pancreatic islet inflammation and  $\beta$ -cell apoptosis. *Diabetes Obes. Metab.* **15**, 71–81 (2013).
67. M. Nogueira, L. Puig, T. Torres, JAK inhibitors for treatment of psoriasis: Focus on selective TYK2 inhibitors. *Drugs* **80**, 341–352 (2020).
68. A. Coomans de Brachène, A. Castela, A. Op de Beeck, R. G. Mirmira, L. Marselli, P. Marchetti, C. Masse, W. Miao, S. Leit, C. Evans-Molina, D. L. Eizirik, Preclinical evaluation of tyrosine kinase 2 inhibitors for human beta-cell protection in type 1 diabetes. *Diabetes Obes. Metab.* **22**, 1827–1836 (2020).
69. T. L. W. Muskardin, T. B. Niewold, Type I interferon in rheumatic diseases. *Nat. Rev. Rheumatol.* **14**, 214–228 (2018).
70. J. Diana, Y. Simoni, L. Furio, L. Beaudoin, B. Agerberth, F. Barrat, A. Lehuen, Crosstalk between neutrophils, B-1a cells and plasmacytoid dendritic cells initiates autoimmune diabetes. *Nat. Med.* **19**, 65–73 (2013).
71. S. J. Richardson, T. Rodriguez-Calvo, I. C. Gerling, C. E. Mathews, J. S. Kaddis, M. A. Russell, M. Zeissler, P. Leete, L. Krogvold, K. Dahl-Jørgensen, M. von Herrath, A. Pugliese, M. A. Atkinson, N. G. Morgan, Islet cell hyperexpression of HLA class I antigens: A defining feature in type 1 diabetes. *Diabetologia* **59**, 2448–2458 (2016).
72. B. O. Roep, F. S. Kleijwegt, A. G. S. van Halteren, V. Bonato, U. Boggi, F. Vendrame, P. Marchetti, F. Dotta, Islet inflammation and CXCL10 in recent-onset type 1 diabetes. *Clin. Exp. Immunol.* **159**, 338–343 (2010).
73. R. Patro, G. Duggal, M. I. Love, R. A. Irizarry, C. Kingsford, Salmon provides fast and bias-aware quantification of transcript expression. *Nat. Methods* **14**, 417–419 (2017).
74. J. Harrow, A. Frankish, J. M. Gonzalez, E. Tapanari, M. Diekhans, F. Kokocinski, B. L. Aken, D. Barrell, A. Zadissa, S. Searle, I. Barnes, A. Bignell, V. Boychenko, T. Hunt, M. Kay, G. Mukherjee, J. Rajan, G. Despicio-Reyes, G. Saunders, C. Steward, R. Harte, M. Lin, C. Howald, A. Tanzer, T. Derrien, J. Chrast, N. Walters, S. Balasubramanian, B. Pei, M. Tress, J. M. Rodriguez, I. Ezkurdia, J. van Baren, M. Brent, D. Haussler, M. Kellis, A. Valencia, A. Reymond, M. Gerstein, R. Guigó, T. J. Hubbard, GENCODE: The reference human genome annotation for The ENCODE Project. *Genome Res.* **22**, 1760–1774 (2012).
75. M. I. Love, W. Huber, S. Anders, Moderated estimation of fold change and dispersion for RNA-seq data with DESeq2. *Genome Biol.* **15**, 550 (2014).
76. G. Korotkevich, V. Sukhov, A. Sergushichev, Fast gene set enrichment analysis. *bioRxiv*, 060012 (2019).
77. M. Kanehisa, S. Goto, KEGG: Kyoto Encyclopedia of Genes and Genomes. *Nucleic Acids Res.* **28**, 27–30 (2000).
78. G. Yu, L.-G. Wang, Y. Han, Q.-Y. He, clusterProfiler: An R package for comparing biological themes among gene clusters. *OMICS J. Integr. Biol.* **16**, 284–287 (2012).
79. S. Heinz, C. Benner, N. Spann, E. Bertolino, Y. C. Lin, P. Laslo, J. X. Cheng, C. Murre, H. Singh, C. K. Glass, Simple combinations of lineage-determining transcription factors prime cis-regulatory elements required for macrophage and B cell identities. *Mol. Cell* **38**, 576–589 (2010).
80. A. Subramanian, R. Narayan, S. M. Corsello, D. D. Peck, T. E. Natoli, X. Lu, J. Gould, J. F. Davis, A. A. Tubelli, J. K. Asiedu, D. L. Lahr, J. E. Hirschman, Z. Liu, M. Donahue, B. Julian, M. Khan, D. Wadden, I. C. Smith, D. Lam, A. Liberzon, C. Toder, M. Bagul, M. Orzechowski, O. M. Enache, F. Piccioni, S. A. Johnson, N. J. Lyons, A. H. Berger, A. F. Shamji, A. N. Brooks, A. Vrcic, C. Flynn, J. Rosains, D. Y. Takeda, R. Hu, D. Davison, J. Lamb, K. Ardlie, L. Hogstrom, P. Greenside, N. S. Gray, P. A. Clemons, S. Silver, X. Wu, W.-N. Zhao, W. Read-Button, X. Wu, S. J. Haggarty, L. V. Ronco, J. S. Boehm, S. L. Schreiber, J. G. Doench, J. A. Bittker, D. E. Root, B. Wong, T. R. Golub, A next generation Connectivity Map: L1000 platform and the first 1,000,000 profiles. *Cell* **171**, 1437–1452.e17 (2017).

#### Acknowledgments

**Funding:** D.L.E. acknowledges the support of a grant from the Welbio-FNRS (Fonds National de la Recherche Scientifique), Belgium, the Dutch Diabetes Fonds (DDFR), Holland, startup funds from the Indiana Biosciences Research Institute (IBRI), Indianapolis, Indiana, USA, and the Innovative Medicines Initiative 2 Joint Undertaking under grant agreement nos. 115797 (INNODIA) and 945268 (INNODIA HARVEST), supported by the European Union's Horizon 2020 Research and Innovation Programme. These Joint Undertakings receive support from the Union's Horizon 2020 research and innovation programme and “EFPIA,” “JDRF,” and “The Leona M. and Harry B. Helmsley Charitable Trust.” C.E.-M. acknowledges the support of NIH grants R01 DK093954, VA Merit Award I01BX001733, JDRF 2-SRA-2018-493-A-B, and JDRF 2-SRA-2019-834-S-B (to C.E.-M. and D.L.E.); M.M. is supported by the JDRF. **Author contributions:** M.L.C., F.S., M.J.M., C.E.-M., and D.L.E. conceived the analysis. M.L.C. and D.L.E. supervised the analysis. F.S. and M.L.C. performed the bioinformatics analyses. F.S., M.L.C., and D.L.E. wrote the manuscript, and all authors revised it. D.L.E. provided the main funding. **Competing interests:** The authors declare that they have no competing interests. **Data and materials availability:** All data needed to evaluate the conclusions in the paper are present in the paper and/or the Supplementary Materials. Raw RNA-seq data are accessible from the GEO repository (<https://ncbi.nlm.nih.gov/geo/>) via their GSE codes as stated in Table 1. sc/sn-RNA-seq data are accessible from the repositories indicated in Materials and Methods (see above). Additional data related to this paper may be requested from the authors.

Submitted 10 July 2020

Accepted 16 November 2020

Published 6 January 2021

10.1126/sciadv.abd7600

**Citation:** F. Szymczak, M. L. Colli, M. J. Mamula, C. Evans-Molina, D. L. Eizirik, Gene expression signatures of target tissues in type 1 diabetes, lupus erythematosus, multiple sclerosis, and rheumatoid arthritis. *Sci. Adv.* **7**, eabd7600 (2021).

## Gene expression signatures of target tissues in type 1 diabetes, lupus erythematosus, multiple sclerosis, and rheumatoid arthritis

F. Szymczak, M. L. Colli, M. J. Mamula, C. Evans-Molina and D. L. Eizirik

*Sci Adv* 7 (2), eabd7600.  
DOI: 10.1126/sciadv.abd7600

ARTICLE TOOLS	<a href="http://advances.sciencemag.org/content/7/2/eabd7600">http://advances.sciencemag.org/content/7/2/eabd7600</a>
SUPPLEMENTARY MATERIALS	<a href="http://advances.sciencemag.org/content/suppl/2021/01/04/7.2.eabd7600.DC1">http://advances.sciencemag.org/content/suppl/2021/01/04/7.2.eabd7600.DC1</a>
REFERENCES	This article cites 79 articles, 13 of which you can access for free <a href="http://advances.sciencemag.org/content/7/2/eabd7600#BIBL">http://advances.sciencemag.org/content/7/2/eabd7600#BIBL</a>
PERMISSIONS	<a href="http://www.sciencemag.org/help/reprints-and-permissions">http://www.sciencemag.org/help/reprints-and-permissions</a>

Use of this article is subject to the [Terms of Service](#)

---

*Science Advances* (ISSN 2375-2548) is published by the American Association for the Advancement of Science, 1200 New York Avenue NW, Washington, DC 20005. The title *Science Advances* is a registered trademark of AAAS.

Copyright © 2021 The Authors, some rights reserved; exclusive licensee American Association for the Advancement of Science. No claim to original U.S. Government Works. Distributed under a Creative Commons Attribution NonCommercial License 4.0 (CC BY-NC).